NIH Public Access
Author Manuscript
Cancer Discov. Author manuscript; available in PMC 2014 July 01.

Published in final edited form as:
Cancer Discov. 2013 July ; 3(7): 782–797. doi:10.1158/2159-8290.CD-12-0215.

Diacylglycerol kinase alpha is a critical signaling node and novel therapeutic target in glioblastoma and other cancers

Charli L. Dominguez[1], **Desiree H. Floyd**[1], **Aizhen Xiao**[1], **Garrett R. Mullins**[2], **Benjamin A. Kefas**[1], **Wenjun Xin**[3], **Melissa N. Yacur**[1], **Roger Abounader**[4], **Jae K. Lee**[3], **Gabriela Mustata Wilson**[5], **Thurl E. Harris**[2], and **Benjamin W. Purow**[1]

[1]Division of Neuro-Oncology, Neurology Department, University of Virginia Health System, Charlottesville, VA 22908

[2]Pharmacology Department, University of Virginia Health System

[3]Division of Biostatistics, Department of Public Health, University of Virginia Health System

[4]Microbiology Department, University of Virginia Health System

[5]College of Nursing and Health Professions, University of Southern Indiana, Evansville, IN 47712

Abstract

While Diacylglycerol kinase alpha (DGKα) has been linked to several signaling pathways related to cancer cell biology, it has been neglected as a target for cancer therapy. The attenuation of DGKα activity via DGKα-targeting siRNA and small-molecule inhibitors, R59022 and R59949, induced caspase-mediated apoptosis in glioblastoma cells and in other cancers, but lacked toxicity in non-cancerous cells. We determined that mTOR and HIF-1α are key targets of DGKα inhibition, in addition to its regulation of other oncogenes. DGKα regulates mTOR transcription via a unique pathway involving cyclic AMP. Lastly, we showed efficacy of DGKα inhibition with shRNA or a small-molecule agent in glioblastoma and melanoma xenograft treatment models, with growth delay and decreased vascularity. This study establishes DGKα as a central signaling hub and a promising therapeutic target in the treatment of cancer.

INTRODUCTION

High-grade gliomas are the most common brain tumors in adults and are universally fatal. These tumors partially resemble glial cells, but their cell of origin is unclear. Glioblastoma multiforme (GBM), grade IV glioma, is the most common and aggressive variant. GBMs are primary cancers of the CNS that appear *de novo* or arise from low-grade gliomas (1) and account for >51% of all gliomas diagnosed each year. GBMs are exceedingly treatment-resistant, even with combined surgical resection and radio- and chemotherapy, and always recur (2). These tumors are highly invasive and infiltrate the normal brain parenchyma in a diffuse fashion, which contributes to their resistance (3). The frequency and lethality of GBM, combined with resistance to treatment, present a critical need for novel therapeutic approaches.

Treatment resistance also arises in GBM and other cancers through their genetic diversity and complexity. It has been shown in cancer, perhaps most elegantly in GBM (4), that

Corresponding Author: Benjamin Purow, University of Virginia Health System, Old Medical School – Room 4881, 21 Hospital Drive, Charlottesville, VA 22908. Phone 434-924-5545, fax 434-243-6843, bwp5g@virginia.edu.

Conflicts of Interest: We have no conflicts of interest to disclose.

NIH-PA Author Manuscript
NIH-PA Author Manuscript
NIH-PA Author Manuscript

NIH-PA Author Manuscript

NIH-PA Author Manuscript

NIH-PA Author Manuscript

multiple signaling pathways are dys-regulated in an individual cell. Thus the inhibition of one or two pathways promotes the up-regulation of other oncogenic pathways—in part through feedback loops—allowing the cancer cell to survive. It is therefore increasingly clear that more effective cancer treatment will require either cocktails of inhibitors or the discovery of critical signaling nodes that can be targeted to block numerous pathways simultaneously. Herein we investigate a possible signaling node as a promising cancer target.

We previously showed Notch to be a potential therapeutic target in glioblastoma (5), and in subsequent efforts to determine its signaling role we have sought to better understand its crosstalk with other pathways. This led us to profile microRNAs regulated by Notch, as we have described previously (6). MiRNA-297 was among the microRNAs found to be up-regulated with Notch inhibition, and upon delivery to glioblastoma cells it was observed to be more toxic than any other miRNA tested in our laboratory. This led us to consider possible targets of miRNA-297. After an extensive search through online databases, we did not find any known oncogenes predicted to be strongly targeted by miRNA-297, but the gene Diacylglycerol kinase alpha was among the top predicted targets.

Diacylglycerol (7) is a membrane lipid that is an established second messenger activating several signaling proteins, most of which have been implicated in cancer (8). DAG is typically metabolized through diacylglycerol kinases (DGKs), resulting in the creation of phosphatidic acid (9). Phosphatidic acid (PA) is a phospholipid that is found at relatively low levels compared to other lipids, yet it has been implicated in regulating a number of signaling pathways and proteins (10). Though there are ten known DGK enzymes, Diacylglycerol kinase alpha (DGKα) has been implicated in a variety of cellular functions apart from other DGKs. Through siRNA knockdown of DGKα, it was shown to play a positive role in the proliferation and migration of endothelial cells (11). DGKα also plays a role in the regulation of NF-κB in melanomas. While DGKα is expressed in several melanoma lines, it is not expressed in noncancerous melanocytes (12). Of note, DGKα synthesis of PA can be attenuated by two established small molecule inhibitors: R59022 {6-[2-[4-[(4-Fluorophenyl)phenylmethylene]-1-piperidinyl]ethyl]-7-methyl-5H-thiazolo-[3,2-a]-pyrimidin-5-one} and R59949 {3-[2-[4-[Bis(4-fluorophenyl)methylene]-piperidin-1-yl]ethyl]-sulfanylidene-1H-quinazolin-4-one}. Both R59022 and R59949 are selective for DGKα and the relative specificity of these inhibitors has been previously demonstrated (13). A recent report showed that the inhibition of DGKα by the small-molecule drug R59949 regulated the build-up of hypoxia-inducible factor-1α (HIF-1α) levels, a response to hypoxia and a hallmark of the tumor microenvironment (14). Another report showed that R59949, a DGKα dominant-negative mutant, and specific RNA interference each inhibited VEGF-induced chemotaxis and DNA synthesis in HUVEC endothelial cells (11). The same study also showed a correlation between VEGF-A stimulation and increasing DGKα levels. All of this taken together poses a mounting case for DGKα regulating cell survival, proliferation, migration, and angiogenesis signaling in a variety of cellular environments. The need for further investigation of DGKα as a possible therapeutic target in cancer is evident, given its numerous connections to oncogenic pathways. Herein we show in GBM and other cancers that DGKα is a critical signaling node essential for several oncogenic pathways and is a promising therapeutic target.

RESULTS

Attenuation of DGKα causes toxicity in glioblastoma cells

To assess the effect of this inhibition in established GBM cell lines, DGKα was silenced with siRNA and inhibited via small-molecule inhibitor, R59022. Percent cell death by trypan blue was significantly increased in both U87 and U251 cell lines when compared to

NIH-PA Author Manuscript

NIH-PA Author Manuscript

NIH-PA Author Manuscript

controls (Fig. 1A). In conjunction with the observed cell toxicity, cell viability by alamarBlue assay was significantly reduced with DGKα silencing in both GBM cell lines (Supplemental Fig. S1). To visualize cell toxicity changes after DGKα knockdown, U251 GBM cells were stained with Hoechst and propidium iodide, revealing a decrease in total cell number with an increase in membrane-compromised cells after DGKα knockdown (Fig. 1B). An immunoblot for DGKα was also done to verify transfection efficiency in both GBM cell lines as well (Fig. 1C). The toxicity seen in GBM cells was consistently observed with relative rapidity after treatment with either siRNA or small-molecule inhibitors targeting DGKα. We sought to confirm that cell death was being induced and by what mechanism. Typically, cell count assays were performed between 72–96 hours post treatment, showing a rapid effect on cell numbers given the typical time course for siRNA knockdown. A slowing in cell proliferation was considered unlikely, given no change in BrdU incorporation measured by ELISA assay (data not shown). Autophagy was also explored, but there was no difference in LC3-II levels by immunoblot (data not shown). To assess the possibility of cell death, Annexin V assay via FACS analysis was performed on the U87 and U251 GBM lines and the A-375 melanoma line (Fig. 1D), with the results indicating an increase in Annexin V-positive cells with DGKα knockdown. Next, caspase-mediated apoptosis was investigated at both 24- and 36-hour time points. After transfection, there was a significant increase in caspase-3/7 activity in cells upon silencing DGKα in U87 and U251 GBM cells, as well as in melanoma cells (Fig. 1E). In addition, we observed an increase in cleaved PARP expression in cell lysates in which DGKα expression was silenced (Fig. 1F). These results suggest that DGKα inhibition causes cell toxicity in cancer cells through caspase-mediated apoptosis.

DGKα is up-regulated and increases cell numbers in human glioblastoma

Next, we sought to determine if DGKα might have oncogenic properties, given the substantial effect that silencing has on GBM cell proliferation. In U87, U251, and A-375 cells, forced over-expression of DGKα by transient transfection resulted in a significant increase in cell proliferation (Fig. 2A). Next, in order to establish long-term over-expression of DGKα, we infected U87, U251, and A-375 cells with a lentiviral DGKα vector. DGKα over-expression significantly increased tumor cell proliferation (Fig. 2B) *in vitro*. Upon quantification of DGKα protein by immunoblot in both normal brain and GBM human tissue samples, we found there to be modest but significant increases in levels of DGKα protein in GBMs (Fig. 2C). Also, both normal and GBM tissue samples were analyzed to determine mRNA levels of DGKα (Fig. 2D). While the difference in mean DGKα mRNA levels was not significant, some GBM samples had markedly increased DGKα mRNA. Lastly, other data available online from the Cancer Genome Atlas (15) indicate amplification of DGKα in 1–4% of GBM and several other cancers (Supplemental Table 1). Nonetheless, the moderate over-expression of DGKα in GBM cells seems inconsistent with the apparent addiction to its expression, suggesting this may be an example of “non-oncogene addiction”—in which cancer cells have a disproportionate dependency on a gene that is not over-expressed (16).

Glioblastoma toxicity is a specific effect of decreased DGKα activity

DGKα produces phosphatidic acid (PA) through the phosphorylation of diacylglycerol. In order to verify that the cellular toxicity observed in GBM cells is a specific consequence of the attenuation of DGKα activity, we investigated the role of PA. Knockdown of DGKα was performed in GBM cells as above and exogenous PA added. Notably, the substantial cytotoxicity in GBM (Fig. 3A and B) and melanoma (Fig. 3C) cells upon DGKα knockdown was rescued with exogenous PA. Similarly, PA administration also rescued the phenotype observed upon treatment with small-molecule inhibitor R59022 (Fig. 3D and E) in GBM cells. Lastly, to confirm that PA levels were decreased with DGKα knockdown, PA

NIH-PA Author Manuscript

NIH-PA Author Manuscript

NIH-PA Author Manuscript

levels were measured through mass spectrometry. Total PA levels were significantly decreased in U251 GBM cells after transfection with DGKα siRNA (Fig. 3F). These results establish a role for DGKα production of PA in cancer cell viability.

Attenuation of DGKα causes toxicity through regulating key oncogenic pathways

DGKα and its product phosphatidic acid have been linked to several established oncogenic pathways, including mTOR (17), HIF-1α (14), and Akt (18). To evaluate the effects that silencing DGKα has on these possible mediators, immunoblots were done in GBM cells with DGKα knockdown. There was a significant decrease in total mTOR and phos-mTOR $_{ser2448}$ in GBM cells (Fig. 4A and B) and melanoma cells with attenuation of DGKα activity (Fig. 4C). HIF-1α and phos-mTOR$_{ser2448}$ were decreased by DGKα knockdown in GBM cells (Fig. 4A) as well. In addition, we found that DGKα knockdown decreases c-Myc levels and phosphorylation of Akt$_{ser473}$ (Supplemental Fig. S2). We were also prompted to assess whether DGKα inhibition influences the SREBP (sterol regulatory element binding protein) cholesterol synthetic pathway by two recent reports, the first linking mTOR and the phosphatidic acid modulator lipin to SREBP activity (19), and the second establishing SREBP as oncogenic and a therapeutic target in GBM (20). Following DGKα knockdown in glioblastoma cells, we determined mRNA levels of the SREBP targets farnesyl diphosphate synthase (FDPS), HMG-CoA reductase (HMGCR), and stearoyl CoA-desaturase (SCD) (19). After normalization, each of the genes tested had significantly reduced mRNA levels when compared to control (Supplemental Fig. S3A). To assess whether any of these DGKα mediators might be central for the cytotoxicity of DGKα knockdown/inhibition in GBM cells, we performed “rescue” experiments with over-expression of wild-type mTOR and constitutively active HIF-1α. Over-expression of mTOR and HIF-1α alone each partially rescued the toxicity from DGKα knockdown and inhibition, and when combined the phenotypic rescue was slightly stronger in both GBM and melanoma cells (Fig. 4D, E, and F). However, a similar over-expression of c-Myc failed to rescue the toxicity (Supplemental Fig. S3B). Taken together, these data suggest that decreased expression of mTOR and HIF-1α play substantial roles in the cytotoxicity observed with DGKα knockdown and inhibition in cancer.

DGKa regulates mTOR transcription through modulation of cyclic AMP levels

A similar degree of phenotypic rescue from DGKα knockdown occurred with a wild-type mTOR expression vector as with a constitutively-active mTOR vector (data not shown). This, combined with a strong correlation of DGKA and mTOR mRNA expression in the TCGA GBM data (Fig. 4G) (Supplemental Table 2), suggested that DGKα might regulate mTOR expression. Given prior reports that PA promotes activity of phosphodiesterases decreasing cyclic AMP (7) and that a cAMP-modulated transcription factor could drive mTOR transcription (21) (22), we hypothesized that DGKα was diminishing cAMP levels to prompt a rise in mTOR transcription. To initially evaluate this, we first assessed the effects on mTOR expression of DGKα knockdown with a lentiviral shRNA. We observed a significant decrease in mTOR mRNA levels with prolonged DGKα knockdown versus control (Fig. 4H). Given this result, we used an mTOR promoter reporter luciferase assay to determine if DGKα transcriptionally regulates mTOR. With attenuation of DGKα activity via siRNA and small-molecule inhibitor, there was a significant decrease in mTOR promoter activity in GBM and melanoma cells (Fig. 4I and J). To evaluate whether DGKα was significantly affecting cAMP levels in GBM cells, ELISA was performed after DGKα activity was attenuated via siRNA and small molecule inhibitor. This revealed significant increases in cAMP levels with DGKα knockdown and inhibition in GBM and melanoma cells (Fig. 4 K and L). To determine if cAMP regulates mTOR transcription in GBM, cells were treated with exogenous cAMP and mTOR promoter activity assessed by luciferase assay; we observed a significant decrease in mTOR transcription (Fig. 4M). In addition,

NIH-PA Author Manuscript

NIH-PA Author Manuscript

NIH-PA Author Manuscript

cells treated with the phosphodiesterase-4D inhibitor rolipram also demonstrated a significant decrease in mTOR transcription (Fig. 4N), further supporting the role of cAMP in the hypothesized pathway (Fig. 4O). These data indicate for the first time that DGKα regulates mTOR transcription, likely via modulating cAMP levels. This novel pathway regulating mTOR expression may have implications not only for the role of DGKα in GBM, but also for studies of the role of cAMP and of mTOR regulation in cancer.

Relative lack of cytotoxicity of targeting DGKa in non-cancerous cells

Classically, one of the disadvantages of therapeutic treatments for cancer is the negative side effects due to nonspecific effects on non-cancerous cells. To assess the effect of DGKα inhibition on non-cancerous cells, we utilized normal human astrocytes and fibroblasts. First, we silenced DGKα expression in astrocytes (Fig. 5A) with siRNA and confirmed transfection efficiency with an immunoblot (Fig. 5B), with no significant effect on cell numbers. We then attempted to assess toxicity of the small-molecule inhibitors on these non-cancerous cells, and similarly did not observe any significant decrease in cell viability at concentrations toxic in GBM lines (Fig. 5C and D). Next, we assessed the role DGKα plays on predicted downstream targets in these non-cancerous cells to determine if the regulation seen above is particular to cancer cell signaling. With attenuation of DGKα activity in astrocytes, we did not observe the increase in cAMP levels seen in GBM cells (Fig. 5E). Furthermore, in astrocytes exogenous cAMP (Fig. 5F) and rolipram (Fig. 5G) did not affect mTOR promoter activity. These data suggest that DGKα knockdown and inhibition are preferentially toxic to cancer cells, possibly in part because a major downstream mechanism in cancer cells is unaffected in normal cells.

DGKα inhibition is cytotoxic in multiple cancer lines

Given the toxicity observed in GBM cell lines, its impact on major oncogenic pathways, the previous report on DGKα over-expression in melanoma cells (12), and its amplification in subsets of several cancers (described above), we sought to determine if DGKα is a potential therapeutic target in other types of cancer as well. First, lysates from various cancer cell lines and normal human astrocytes and fibroblasts were evaluated by immunoblot to assess the basal DGKα levels in each cell line used in this work (Fig. 6A). Also, in melanoma (Fig. 6B), cervical (Fig. 6C), and breast (Fig. 6D) cancer cell lines the percent cell death after knockdown of DGKα or inhibition via small-molecule inhibitor R59022 (10 μM) was assessed by trypan blue cell counts. Second, to evaluate the potential therapeutic window of the small-molecule inhibitor R59022, we conducted a dose response assay in each cancer and normal cell line used above. Each cell line was treated with doses ranging from 5 μM to 100 μM, with DMSO (volume:volume) controls at each dose. Percent cell survival was evaluated at 4 days for each dose and dose-response curves plotted (Fig. 6E). Cancer cell lines were substantially more sensitive to R59022 than normal cells.

DGKα knockdown and inhibition affect tumor growth, angiogenesis, and survival of mice with intracranial and subcutaneous tumors

To test DGKα knockdown as a potential therapy, we first utilized a GBM stem cell (GSC) xenograft treatment model in mice. DGKα knockdown via lentiviral vector was tested against a GSC line *in vitro* (Supplemental Fig. S4) and *in vivo*. First, 0308 GSCs were stereotactically injected into the brain of immunodeficient SCID mice and given a week to become established. Lentiviral particles containing control or DGKα shRNA were delivered via convection-enhanced delivery, to increase delivery volume and to promote diffusion of the virus. The treatment group had significantly increased survival (p= .0073) (Fig. 7A), and MRI images also showed significantly smaller tumor size in this group as well (Fig. 7B).

NIH-PA Author Manuscript

NIH-PA Author Manuscript

NIH-PA Author Manuscript

To predict whether one of the small-molecule DGKα inhibitors would penetrate the blood-brain barrier (BBB) sufficiently, we utilized an in silico algorithm based on the BBB penetration of hundreds of diverse compounds in rodents. This algorithm predicted that R59022 would have adequate BBB penetration while R59949 would not, despite their very similar structures (Figure 7C) (Supplemental Table 3) (23).

Next, the DGKα small-molecule inhibitor R59022 was utilized *in vivo* to initially evaluate the therapeutic potential of systemic DGKα inhibition. SCID mice were implanted with U87 GBM cells by the techniques above. After tumor establishment, mice were given daily intraperitoneal injections of either DMSO or 2mg/kg of R59022 for 12 consecutive days. The treatment group had significantly increased survival (p=.01) (Fig. 7D). It is important to note that there was no decrease in mouse weights with R59022 treatment at doses of 2 or 10 mg/kg (data not shown).

To further evaluate the effects of R59022 administration, U87 GBM cells were injected into the flank of nude mice to establish subcutaneous tumors. Daily injections were given as above, and we noted that mean tumor volumes were significantly smaller after treatment with the DGKα inhibitor (Fig. 7E) (Supplemental Table 4A). When we allowed some tumors from mice treated with R59022 time to catch up in size with tumors from DMSO-treated mice, the resected tumors displayed an obvious difference in vascularity (Fig. 7F). Given this change in vascularity, immunohistochemistry for CD34 was performed to visualize blood vessels at the microscopic level. There was a sharp decrease in blood vessel density in the treated tumors (representative image in Fig. 7G). To assess for apoptosis in these resected tumors, immunohistochemistry for cleaved Caspase-3 (Fig. 7H) was performed, indicating clear signs of apoptosis in tumors after DGKα inhibition.

To determine if systemic DGKα inhibition might have therapeutic potential against other cancers, we also tested it with subcutaneous implantation of A-375 melanoma cells. After daily intraperitoneal injections with the inhibitor R59022, mean tumor volume of treated mice was significantly smaller in comparison to control mice (Fig. 7I) (Supplemental Table 4B).

Lastly, as the DGKα small-molecule inhibitors have not previously been evaluated *in vivo*, we performed an initial pharmacokinetic study. Blood plasma levels of R59022 were evaluated via mass spectrometry at several time points after a single intraperitoneal dose of 10 mg/kg. These studies revealed a short-half life and peak concentration at 2 hours (Fig. 7J). Ongoing studies are being conducted to further evaluate the pharmacokinetics and explore the pharmacodynamics of this drug. These results underscore the potential of DGKα as a therapeutic target, since significant benefit was observed with just a single local infusion of lentiviral shRNA or short course of a small-molecule inhibitor. Optimized delivery of DGKα inhibitors *in vivo* could greatly enhance their efficacy against GBM and other cancers.

DISCUSSION

While previous reports have linked DGKα to specific cellular pathways, this research has largely focused on lipid cellular signaling (24) (25) or immunology (26). This kinase has yet to receive significant attention for its impact on cancer cell viability and its potential as a cancer target. Notably, one recent report establishes a key role for DGKα in cancer cell migration, and even more recently it was noted that DGKα restrains the anti-tumor immune response (27). Our work establishes DGKα as a promising therapeutic target for the treatment of GBM, with potential for other cancers as well. The attenuation of DGKα through siRNA, shRNA, and small-molecule inhibitors all produce striking cellular toxicity

NIH-PA Author Manuscript

NIH-PA Author Manuscript

NIH-PA Author Manuscript

in GBM cells, as well as in other cancers. Conversely, overexpression of this kinase promotes GBM cell proliferation *in vitro*, and expression levels are moderately increased in human GBM tissue samples. DGKα thus exhibits oncogene-like characteristics; however, the increase in DGKα expression is moderate, suggesting the possibility of a cancer-specific non-oncogene addiction and not a classic oncogenic model. The non-oncogene addiction model suggests that certain genes, while not significantly over-expressed in cancer, are nonetheless far more necessary for the survival of cancer cells than normal cells and can represent promising therapeutic targets (16, 28). That being said, profiling studies such as TCGA have indicated amplification of the DGKα locus in 1–4% of several cancers, as noted above. Further studies, with higher sample numbers, need to be done to assess expression levels of DGKα in patient samples of GBM and other cancers to help clarify its degree of over-expression.

The history of cancer research is rife with examples of promising therapeutic strategies that proved disappointing in patients. This is due in large part to the genetic instability and heterogeneity of cancer cells, which render them able to develop resistance to treatments and adapt cellular networks to maintain a malignant phenotype (29). This seems especially likely for therapies directed toward a single target or pathway, as in therapies specifically targeting angiogenesis (30) or tyrosine kinases (31). Targeting a signaling node such as DGKα, with critical roles in numerous key cancer pathways, represents one answer to these obstacles. We have shown that inhibition of DGKα decreases the expression and/or phosphorylation of mTOR (32), HIF-1α (33), Akt (34), and c-Myc (35). We hypothesized that regulation of these key oncogenic pathways underlies the cytotoxicity of DGKα inhibition. To assess their relative importance, we delivered mTOR, HIF-1α, and c-Myc plasmids to GBM cells treated with DGKα inhibition. Both mTOR and HIF-1α plasmids partially rescued cell toxicity, and even more so when combined. While inhibition of mTOR and HIF1-α were critical in mediating DGKα inhibition in GBM cells, it is important to note that other pathways may be more central in other cancers; DGKα has been shown by others to mediate Ras/Raf (36), ALK (37), Met (11), and VEGF (11) signaling. Furthermore, we found a link between DGKα inhibition and the transcriptional regulator SREBP (38), which has recently been found to promote tumor growth in GBM patients through the PI3K/AKT signaling pathway (20). After DGKα silencing, mRNA expression of several genes induced by SREBP were significantly decreased. It is notable that SREBP has also been linked to mTOR and PA signaling, which suggests that DGKα may regulate SREBP via more than one pathway. While the intricacies of the mechanisms through which DGKα inhibition exerts its toxic effects on different cancers need further investigation, we are optimistic that this approach may damage too many oncogenic pathways for cancer cells to adapt to treatment.

We were initially surprised to see equally strong rescue in cancer cell toxicity from DGKα inhibition with expression vectors for mTOR and constitutively-active mTOR (data not shown). This, along with a strong correlation between DGKα and mTOR expression levels in TCGA GBM samples, suggested that DGKα might be regulating mTOR expression as well as activity. Further experiments supported this, via a unique DGKα—PA—PDE—cAMP—mTOR transcription pathway. This appears to be a significant function for DGKα in cancer cells. These results have importance not only for neuro-oncology, but also for the study and targeting of cAMP and mTOR in cancer. It indicates a new approach to mTOR inhibition, using small-molecule DGKα inhibitors to decrease mTOR expression. Reducing mTOR expression may have advantages over mTOR inhibitors now in use that inhibit mTORC1 and/or mTORC2, given that mTOR has been hypothesized to participate in an mTORC3 complex and may have other pro-cancer functions as well. DGKα inhibition also seems to represent a novel cancer-specific means to elevate cAMP levels selectively in cancer cells, potentially avoiding side effects from non-selective cAMP-elevating agents

NIH-PA Author Manuscript

NIH-PA Author Manuscript

NIH-PA Author Manuscript

such as phosphodiesterase inhibitors. In addition, these findings are likely to have implications for other signaling pathways in cancer that also regulate cAMP levels.

Most successful cancer treatments have a broad therapeutic window, i.e. they affect cancer cells at much lower concentrations than they do normal cells. The ideal treatment would pose little risk to normal cells while efficiently killing cancer cells. It is important to note that DGKα inhibition significantly affects cell viability in normal human cells only at very high concentrations, suggesting there may be a substantial therapeutic window *in vivo*. The minimal effect in non-cancerous cells, combined with the marked toxicity in GBM cells, also points to the possibility of cancer cells having a dependence on DGKα that is not seen in normal cells. Though there have been ten DGK enzymes discovered to date, there does not seem to be functional redundancy and DGKα seems to be particularly relevant for cancer cells. For example, it has been shown that normal melanocytes do not express DGKα, while melanoma cells do express this isoform (12). It is notable that DGKα knockout mice are generally healthy, with a defect in T cell anergy (39). Our *in vivo* experiments supported the potential safety of using DGKα small-molecule inhibitors, as no toxicity was observed and there was no decrease in mouse weights with R59022 treatments at doses of 2 or 10mg/kg (data not shown). While promising in these preliminary studies, the safety profile of DGKα inhibition needs to be evaluated with detailed animal studies.

These results also showed the utility of a single injection of DGKα-targeted therapy in a challenging GBM treatment model, using highly-invasive and resistant GSCs. Convection-enhanced delivery (CED) was utilized for the infusion of lentiviral particles carrying DGKα shRNA, in a manner that could be clinically applicable. The shRNA targeting DGKα was delivered in lentiviral particles to achieve long-term expression (40). The fact that DGKα knockdown through a single infusion had a significant effect on tumor growth *in vivo* is encouraging, and it is likely that repeated treatment with DGKα inhibition would result in improved efficacy.

The therapeutic potential of DGKα inhibition is facilitated by its being druggable, with two compounds already available. While it is always possible with small-molecule agents such as R59022 and R59949 that nonspecific effects contributed to their toxicity in cancer cells, the PA-replacement rescue experiments shown here argue against this. Initial *in vivo* experiments supported the therapeutic potential of these DGKα small-molecule inhibitors. This was true in both orthotopic and subcutaneous GBM models, as well as in a subcutaneous melanoma model. Our experiments also suggested that this *in vivo* efficacy might have been due at least in part to potent antiangiogenic effects. Pharmacokinetic studies indicated that the positive *in vivo* results were obtained despite a short R59022 half-life in the mouse. It is possible that R59022 accumulates in the tumor with repeated dosing, or that tumor cells are sensitive to lower concentrations *in vivo* than they are *in vitro*. We demonstrate that R59022 exhibits a pronounced anti-angiogenic effect *in vivo*, and this may occur at lower concentrations than what was utilized *in vitro*. Regardless of mechanism, the pharmacokinetic data suggest that better efficacy could be achieved with DGKα inhibitors optimized for *in vivo* usage.

We propose that this work sets the foundation for DGKα as a promising therapeutic target in cancer. These results shed light on the significant effects of DGKα inhibition on cancer cell viability, the possibility it is an oncogene or example of non-oncogene addiction, and its safety for normal cells. Our results establish DGKα as a single therapeutic target linked to multiple oncogenic pathways, with relevance for GBM and other cancers as well. This work also indicates the importance of the DGKα product PA in cancer cell biology, and ongoing studies are evaluating this signaling phospholipid as a therapeutic target in itself.

NIH-PA Author Manuscript

NIH-PA Author Manuscript

NIH-PA Author Manuscript

METHODS

Cell lines and patient samples

U87MG, MDA-MB-231, HeLa, and human fibroblast cell lines were obtained from ATCC (Manassas, VA). U251MG was a gift of Howard Fine (New York University). A-375 was a gift of Daniel Gioeli (University of Virginia). Astrocytes were purchased from Lonza (Walkersville, MD). The tumor stem cell line 0308 was derived and validated as described previously (41). All cell lines were maintained in a 37°C incubator with 5% CO_2. Patient samples were obtained from the Tumor Bank at the University of Virginia under an approved IRB protocol. The cancer lines U87, U251, A-375, MDA-MB-231, and HeLa were authenticated by STR profiling in 2013 by Laragen, Inc. (Culver City, CA). The GBM stem cell line 0308 is a primary line and therefore cannot be authenticated but is used at low-passage number (<15 passages from its initial stocks) in these experiments. The normal human fibroblasts and astrocytes are from a commercial vendor and as primary cells authentication does not apply.

Cell transfection

The effects of DGKα knockdown by siRNA were examined in U251MG (GBM), U87MG (GBM), 0308 (GBM stem cell), A-375 (melanoma), MDA-MB-231 (breast cancer), and HeLa (cervical cancer) cell lines. Cells were plated in six-well tissue culture plates at a density of between $4.0 \times 10^4 – 6.0 \times 10^4$ per well and transfected 24 hours later. Cells were transfected with Oligofectamine (Invitrogen) according to the manufacturer's protocol, with a concentration of 10nmol/L siRNA.

Immunoblots

Immunoblots were performed as previously described (5) Primary antibodies included DGKα (ProteinTech), phospho-AKT, HIF-1α, phos-mTOR, c-Myc, and PARP. All antibodies were obtained from Cell Signaling unless otherwise noted. Horseradish peroxidase-conjugated secondary antibodies to rabbit or mouse immunoglobulin G were used (1:7500, Jackson Immunology Labs, Bar Harbor, ME).

Annexin V Staining

Cells were harvested 4 days post-transfection and Annexin V staining was performed according to the manufacturer's description (BD Biosciences, San Jose, CA).

Caspase 3/7 assay

Cells were harvested with trypsin (Fisher MediaTech, Pittsburgh, PA). Caspase 3/7 assay was performed according to the manufacturer's description (Promega Madison, WI). After one-hour incubation at 25°C, each sample was measured in a Promega Glomax 20/20 Luminometer.

Real-time quantitative PCR

Cells were lysed using Qiazol (Qiagen) and then transferred to QIAshredder columns (Qiagen) and centrifuged at 10,000 g for 3 minutes, then RNA isolated using the RNeasy kit according to the manufacturer's instructions (Qiagen). RT-PCR on 500 ng of RNA using the miScript reverse transcription kit (Qiagen) was used to generate cDNA. From 100 ng of cDNA template, quantitative real-time PCR analyses for FDPS1, FDPS2, HMGCR, SCD, DGKα, and 18S were performed using their specific forward primers and reverse primers according to the manufacturer's protocol (Qiagen). 18S was used as a control. Applied Biosystems (StepOnePlus) real-time PCR system was used to carry out the quantitative PCR, using hot start 95°C (15m), then denaturation 95°C (15s) with annealing at 58°C (30s),

NIH-PA Author Manuscript

NIH-PA Author Manuscript

NIH-PA Author Manuscript

extension 72°C (30s) for 40 cycles, followed by a melt curve analysis. Data analysis for differences in gene expression between control and treated cells, or normal and GBM tissue, was carried out using Microsoft Excel: housekeeping gene primer Ct values were subtracted from test primer values to find the ΔΔCt, then ΔΔCt was found by subtracting the average ΔCt of the vehicle-treated sample from itself and the drug-treated samples. Fold change was calculated using the formula Fold Change = $2^{-\Delta\Delta Ct}$.

Phosphatidic acid rescue experiments

U251MG and U87MG were transfected or treated with small-molecule inhibitors as above. Simultaneously, exogenous phosphatidic acid (Avanti Polar Lipids, Alabaster, AL) at either 33 μM or 50 μM and vehicle (v:v) of a 1:2 methanol and chloroform solution were administered. Treatment was repeated every 24 hours.

Cellular lipid extraction and LPA, PA, and DAG profile assays

Total lipid was extracted from GBM cells by methods described previously (43–45). The cellular content of DAG, LPA and PA profiles was analyzed by LC/MS on a Shimadzu Prominence UFLC (Ultra Fast Liquid Chromatography) system equipped with a C8 column (Nucleodur 5 μm, 2 × 125 mm, Machery-Nagel) and detection was carried out using an Applied Biosystems 4000 Q Trap triple quadrupole LC/MS/MS system equipped with an electrospray ionization system. For PA and LPA, multiple reaction monitoring protocols in negative mode were developed for each phosphatidic acid using commercial pure phosphatidic acids and the most intense product ions were selected for the analysis of biological samples. For DAG, analyses were carried out by monitoring product ions generated by neutral loss (43) of ammoniated acyl groups [RCOOH + NH_3] from DAG's ammonium adducts $[M + NH_4]^+$ as previously described (46). Quantitative methods for the measurement of glycerolipids were performed using the chromatographic and spectrometric methods described above in conjunction with the use of 0.1 nmol C17 LPA and C17 ceramide as an internal standard, for LPA/PA and DAG respectively, to correct for recovery and the protein concentration of the cellular lysates. The amount of each species of glycerolipid in biological samples was calculated from the peak areas obtained using the software that controls the LC/MS system (Analyst 1.5, Applied Biosystems). Raw peak areas were corrected for recovery and sample loading as described above and then transformed into amounts of analyte using standard curves made with commercial glycerolipids.

cAMP assay

The cells were treated with DGK-α inhibitor R59022 (Sigma-Aldrich) at 10μM for 5 days or transfected with DGK-α siRNA. cAMP concentration were determined in cell lysates from cell culture of 3.5×10^5 cells using commercially available assay (cAMP competitive Elisa kit; Thermo Scientific, Rockford, IL) following the manufacturer's instructions. The assay is based on the competition between cAMP in the standard or sample and Alkaline Phosphatase conjugate cAMP (cAMP-AP) for a limited amount of cAMP monoclonal antibody bound to an Anti-Rabbit lgG pre-coated 96 well plate. The assay is colorimetric, and absorbance is read at 405 nm.

Luciferase assay

The cells were transfected with DGKα siRNAs for 4 hours using oligofectamine or treated with DGKα inhibitor R59022 10 μM, PDE4 inhibitor rolipram 40 μM, exogenous cAMP 20 or 80 pmol for 3 days and subsequently transfected with β-galactosidase (2 ng/ul), mTOR promoter luciferase reporter or empty promoter vector (Switchgear Genomics Inc., Menlo Park, CA) following the manufacturer's instructions for 48 hours. Luciferase assays for

NIH-PA Author Manuscript

NIH-PA Author Manuscript

NIH-PA Author Manuscript

mTOR activity were performed using the LightSwitch Assay System (Switchgear Genomics Inc.) and for β-galactosidase activity using Galacto-Light Plus™ beta-Galactosidase Reporter Gene Assay System (Applied Biosystems, Carlsbad, CA). Luminescence was measured on a Promega GloMax 20/20 luminometer and normalized as described previously (6). mTOR luciferase activities were double-normalized by dividing each well by both β-galactosidase activity and the average luciferase/β-galactosidase value in a parallel set done with constitutively-expressed luciferase expression vector.

Pharmacological reagents

The small molecule inhibitors R59022 {6-[2-[4-[(4-Fluorophenyl)phenylmethylene]-1-piperidinyl]ethyl]-7-methyl-5H-thiazolo-[3,2-a]-pyrimidin-5-one} and R59949 {3-[2-[4-[Bis(4-fluorophenyl)methylene]-piperidin-1-yl]ethyl]-sulfanylidene-1H-quinazolin-4-one} were obtained from Sigma-Aldrich (St. Louis, MO).

Small interfering RNA (siRNA) duplexes were synthesized by Sigma-Aldrich (St. Louis, MO). Oligofectamine (Invitrogen) was used for transfection of siRNA into cells per manufacturer's instructions and as previously described (5). siRNA sequence was as follows: DGKα: 5' GGAUUGACCCUGUUCCUAA

Estimates of blood-brain barrier penetration of small-molecule inhibitors

R59022 and R59949 were evaluated for their predicted ability to cross the blood-brain barrier (BBB) using the ACD/ADME software (ACD Labs, Toronto, Canada) (47). The module used for predictions is Pharma Algorithms (23), which provides a comprehensive evaluation of blood-brain barrier penetration potential of compounds in rodents. Each compound of interest is given an estimate whether it would be permeable enough to exhibit CNS activity. Qualitative classification is based on reliable and theoretically reasonable predictions of the rate and extent of BBB permeation (expressed as LogPS and LogBB constants respectively) governed by passive diffusion.

LogBB predictive model is based on a data-set containing >500 brain to plasma partitioning ratios (expressed as LogBB constants) measured in mice and rats. Under the assumption of passive transport across the BBB, LogBB is viewed as a cumulative effect of drug binding to plasma and brain constituents. Calculations therefore use octanol/water logP (main determinant of brain tissue binding) and unbound fraction in plasma (fu, plasma) as input parameters. LogPS module provides more detailed output of the ionization-specific predictive model of BBB permeability in rats. The model was developed using in-vivo experimental data of rates of passive diffusion across BBB for >200 compounds, expressed as LogPS constants. Calculations are performed using essential physicochemical properties such as lipophilicity, ionization constants, hydrogen bonding parameters, and molecular size (calculated or experimental if available) as inputs (23).

In vivo treatment models

Mouse protocols were approved by the IACUC committee at the University of Virginia. Eight-week-old male SCID/NCr Balb/C mice (from NCI) were stereotactically implanted with 25,000 0308 GBM stem cells in 10 μL of Neurobasal media. The surgical procedure was done as described previously (6). Convection-enhanced delivery of lentiviral particles (Sigma-Aldrich) containing shRNA was done at 7 days post-implantation. Animals were randomly divided into 2 groups: control group (7 mice) receiving control shRNA and treatment group (6 mice) receiving DGKα shRNA. Convection-enhanced delivery (CED) was done using the same coordinates as for the tumor implantation. The CED volume was 10 μL as well, at a speed of 300nL/min. The solution also contained 1:2000 polybrene and 7.5% mannitol to promote spread of infusate. General appearance, neurologic status, and

NIH-PA Author Manuscript

NIH-PA Author Manuscript

NIH-PA Author Manuscript

body weight were monitored daily, and mice were euthanized when they demonstrated signs of illness, pain, or 20% weight loss.

Alternatively, following the same protocol mentioned above, 100,000 U87 GBM cells were implanted in 10 μL of DMEM media. Beginning at 7 days post-implantation of tumor cells, mice were given daily intraperitoneal injections with either DMSO (v:v), 2 mg/kg, or 10 mg/kg of R59022 dissolved in DMSO in 50 μL volume.

Immunohistochemistry

Immunohistochemical staining with anti-CD34 antibody (EMD Millipore, Billerica, MA) and anti-cleaved caspase-3 antibody (EMD Millipore), with horseradish peroxidase-conjugated secondary antibody, was done on frozen mounted slices by the University of Virginia Biorepository and Tissue Research Facility using standard techniques.

Plasma R59022 extraction and quantitation

R59022 was extracted from mouse plasma using a modified Bligh-Dyer extraction method. To a 5 mL polypropylene tube containing 100 μl of sample, 500 μl methanol (MeOH), 250 μl chloroform ($CHCl_3$), and 100 μl dH_2O were added, mixed, and incubated on ice for 30 min. To extract, 250 μl $CHCl_3$ and 200 μl 0.2 M sodium chloride (NaCl) were added. The organic phase was dried and suspended in 100 μl of a mixture of $CHCl_3$:MeOH (1:1), and 50 μl was injected into a Shimadzu LC-20AD LC system equipped with a Discovery (Supelco) C18 column (50mm × 2.1 mm, 5 μm bead size). The LC was coupled to a triple quadrupole mass spectrometer (Applied Biosystems 4000 Q-Trap). R59022 was measured in positive mode using the following transition: 460.3 →193.1. Mass spectrometer settings, obtained by direct infusion of a 1 μM solution in Solvent B, were as follows: DP: 66, EP: 10, CE:43, CXP: 14; Ion spray voltage: 5500; Temperature: 500; Curtain gas; 40. Chromatography was carried out using a mobile phase A consisting of 79% H_2O, 20% MeOH, 1% formic acid; and a mobile phase B consisting of 99% MeOH, 1% formic acid. The solvent gradient was as follows: 0.5 min 100% solvent A, a linear gradient to reach 100% solvent B at 5.6 min, 4.3 min 100% solvent B, 1 min 100% solvent A. Total flow was 1 ml/min. Retention time was 3.9 min. Quantification was carried out by measuring peak areas using commercial software (Analyst 1.5.1).

Statistics

In vitro experimental results were analyzed by two-tailed Student's t-test and plotted with Microsoft Excel (Microsoft Corp, Redmond, CA). The *in vivo* experimental results were analyzed using the Kaplan-Meier function utilizing both the Log-rank (Mantel-Cox) test and the Gehan-Breslow-Wilcoxon test in GraphPad Prism 5 (GraphPad Software, Inc., San Diego, CA). Refutation of the null hypothesis was accepted for p-values of less than 0.05. Error bars indicate standard deviation from the mean in all figures.

Supplementary Material

Refer to Web version on PubMed Central for supplementary material.

Acknowledgments

We would like to thank Dr. Gregg Semenza for the constitutively-active HIF-1α plasmid, and Dr. Fadila Guessous and Dr. Ying Zhang for assistance with *in vivo* techniques.

This work was supported in part by NIH R01 CA136803 (B.P.).

NIH-PA Author Manuscript

NIH-PA Author Manuscript

NIH-PA Author Manuscript

References

1. Cerami E, Demir E, Schultz N, Taylor BS, Sander C. Automated network analysis identifies core pathways in glioblastoma. PLoS One. 2010; 5:e8918. [PubMed: 20169195]
2. Adamson C, Kanu OO, Mehta AI, Di C, Lin N, Mattox AK, et al. Glioblastoma multiforme: a review of where we have been and where we are going. Expert Opin Investig Drugs. 2009; 18:1061–1083.
3. Hadjipanayis CG, Van Meir EG. Brain cancer propagating cells: biology, genetics and targeted therapies. Trends Mol Med. 2009; 15:519–530. [PubMed: 19889578]
4. Stommel JM, Kimmelman AC, Ying H, Nabioullin R, Ponugoti AH, Wiedemeyer R, et al. Coactivation of receptor tyrosine kinases affects the response of tumor cells to targeted therapies. Science. 2007; 318:287–290. [PubMed: 17872411]
5. Purow BW, Haque RM, Noel MW, Su Q, Burdick MJ, Lee J, et al. Expression of Notch-1 and its ligands, Delta-like-1 and Jagged-1, is critical for glioma cell survival and proliferation. Cancer Res. 2005; 65:2353–2363. [PubMed: 15781650]
6. Kefas B, Comeau L, Floyd DH, Seleverstov O, Godlewski J, Schmittgen T, et al. The neuronal microRNA miR-326 acts in a feedback loop with notch and has therapeutic potential against brain tumors. J Neurosci. 2009; 29:15161–15168. [PubMed: 19955368]
7. Derrick M, Krakauer D, Magill S, Mikunas D, Musgrave B Jr, et al. The ZEUS Leading Proton Spectrometer and its use in the measurement of elastic rho(0) photoproduction at HERA. Z Phys C Part Fields. 1997; 73:253–268.
8. Topham MK. Signaling roles of diacylglycerol kinases. J Cell Biochem. 2006; 97:474–484. [PubMed: 16288460]
9. Merida I, Avila-Flores A, Merino E. Diacylglycerol kinases: at the hub of cell signalling. Biochem J. 2008; 409:1–18. [PubMed: 18062770]
10. Sakane F, Imai S, Kai M, Yasuda S, Kanoh H. Diacylglycerol kinases: why so many of them? Biochim Biophys Acta. 2007; 1771:793–806. [PubMed: 17512245]
11. Baldanzi G, Mitola S, Cutrupi S, Filigheddu N, van Blitterswijk WJ, Sinigaglia F, et al. Activation of diacylglycerol kinase alpha is required for VEGF-induced angiogenic signaling in vitro. Oncogene. 2004; 23:4828–4838. [PubMed: 15122338]
12. Yanagisawa K, Yasuda S, Kai M, Imai S, Yamada K, Yamashita T, et al. Diacylglycerol kinase alpha suppresses tumor necrosis factor-alpha-induced apoptosis of human melanoma cells through NF-kappaB activation. Biochim Biophys Acta. 2007; 1771:462–474. [PubMed: 17276726]
13. Jiang Y, Sakane F, Kanoh H, Walsh JP. Selectivity of the diacylglycerol kinase inhibitor 3-[2-(4-[bis-(4-fluorophenyl)methylene]-1-piperidinyl)ethyl]-2, 3-dihydro-2-thioxo-4(1H)quinazolinone (R59949) among diacylglycerol kinase subtypes. Biochem Pharmacol. 2000; 59:763–772. [PubMed: 10718334]
14. Temes E, Martin-Puig S, Acosta-Iborra B, Castellanos MC, Feijoo-Cuaresma M, Olmos G, et al. Activation of HIF-prolyl hydroxylases by R59949, an inhibitor of the diacylglycerol kinase. J Biol Chem. 2005; 280:24238–24244. [PubMed: 15849364]
15. Cerami E, Gao J, Dogrusoz U, Gross BE, Sumer SO, Aksoy BA, et al. The cBio cancer genomics portal: an open platform for exploring multidimensional cancer genomics data. Cancer Discov. 2012; 2:401–404. [PubMed: 22588877]
16. Luo J, Solimini NL, Elledge SJ. Principles of cancer therapy: oncogene and non-oncogene addiction. Cell. 2009; 136:823–837. [PubMed: 19269363]
17. Foster DA. Phosphatidic acid signaling to mTOR: signals for the survival of human cancer cells. Biochim Biophys Acta. 2009; 1791:949–955. [PubMed: 19264150]
18. Yalcin A, Clem B, Makoni S, Clem A, Nelson K, Thornburg J, et al. Selective inhibition of choline kinase simultaneously attenuates MAPK and PI3K/AKT signaling. Oncogene. 2010; 29:139–149. [PubMed: 19855431]
19. Peterson TR, Sengupta SS, Harris TE, Carmack AE, Kang SA, Balderas E, et al. mTOR complex 1 regulates lipin 1 localization to control the SREBP pathway. Cell. 2011; 146:408–420. [PubMed: 21816276]

NIH-PA Author Manuscript

NIH-PA Author Manuscript

NIH-PA Author Manuscript

20. Guo D, Reinitz F, Youssef M, Hong C, Nathanson D, Akhavan D, et al. An LXR agonist promotes GBM cell death through inhibition of an EGFR/AKT/SREBP-1/LDLR-dependent pathway. Cancer Discov. 2011; 1:442–456. [PubMed: 22059152]
21. Nemoz G, Sette C, Conti M. Selective activation of rolipram-sensitive, cAMP-specific phosphodiesterase isoforms by phosphatidic acid. Molecular Pharmacology. 1997; 51:242–249. [PubMed: 9203629]
22. Sheng Z, Ma LY, Sun JYE, Zhu LHJ, Green MR. BCR-ABL suppresses autophagy through ATF5-mediated regulation of mTOR transcription. Blood. 2011; 118:2840–2848. [PubMed: 21715304]
23. Japertas P, Didziapetris R, Petrauskas A. Fragmental methods in the analysis of biological activities of diverse compound sets. Mini Rev Med Chem. 2003; 3:797–808. [PubMed: 14529499]
24. Kanoh H, Yamada K, Sakane F, Imaizumi T. Phosphorylation of diacylglycerol kinase in vitro by protein kinase C. Biochem J. 1989; 258:455–462. [PubMed: 2539807]
25. Tyagi MG, Shanthi M, Keshavan V, Vikram GS. Phospholipid mediators and MgATPase modulation causes changes in the cardiovascular effects of vasopressin in lithium carbonate-induced polyuric rats. Methods Find Exp Clin Pharmacol. 2004; 26:257–262. [PubMed: 15319803]
26. Olenchock BA, Guo R, Carpenter JH, Jordan M, Topham MK, Koretzky GA, et al. Disruption of diacylglycerol metabolism impairs the induction of T cell anergy. Nat Immunol. 2006; 7:1174–1181. [PubMed: 17028587]
27. Rainero E, Caswell PT, Muller PA, Grindlay J, McCaffrey MW, Zhang Q, et al. Diacylglycerol kinase alpha controls RCP-dependent integrin trafficking to promote invasive migration. J Cell Biol. 2012; 196:277–295. [PubMed: 22270919]
28. Solimini NL, Luo J, Elledge SJ. Non-oncogene addiction and the stress phenotype of cancer cells. Cell. 2007; 130:986–988. [PubMed: 17889643]
29. Weinstein IB, Joe A. Oncogene addiction. Cancer Res. 2008; 68:3077–3080. discussion 3080. [PubMed: 18451130]
30. Young R, Reed M. Anti-angiogenic Therapy: Concept to Clinic. Microcirculation. 2011
31. Rich JN, Reardon DA, Peery T, Dowell JM, Quinn JA, Penne KL, et al. Phase II trial of gefitinib in recurrent glioblastoma. J Clin Oncol. 2004; 22:133–142. [PubMed: 14638850]
32. Avila-Flores A, Santos T, Rincon E, Merida I. Modulation of the mammalian target of rapamycin pathway by diacylglycerol kinase-produced phosphatidic acid. J Biol Chem. 2005; 280:10091–10099. [PubMed: 15632115]
33. Semenza GL. HIF-1: mediator of physiological and pathophysiological responses to hypoxia. J Appl Physiol. 2000; 88:1474–1480. [PubMed: 10749844]
34. Suzuki Y, Shirai K, Oka K, Mobaraki A, Yoshida Y, Noda SE, et al. Higher pAkt expression predicts a significant worse prognosis in glioblastomas. J Radiat Res (Tokyo). 2010; 51:343–348. [PubMed: 20410674]
35. Flores I, Jones DR, Cipres A, Diaz-Flores E, Sanjuan MA, Merida I. Diacylglycerol kinase inhibition prevents IL-2-induced G1 to S transition through a phosphatidylinositol-3 kinase-independent mechanism. J Immunol. 1999; 163:708–714. [PubMed: 10395661]
36. Rizzo MA, Shome K, Watkins SC, Romero G. The recruitment of Raf-1 to membranes is mediated by direct interaction with phosphatidic acid and is independent of association with Ras. J Biol Chem. 2000; 275:23911–23918. [PubMed: 10801816]
37. Bacchiocchi R, Baldanzi G, Carbonari D, Capomagi C, Colombo E, van Blitterswijk WJ, et al. Activation of alpha-diacylglycerol kinase is critical for the mitogenic properties of anaplastic lymphoma kinase. Blood. 2005; 106:2175–2182. [PubMed: 15928040]
38. Bengoechea-Alonso MT, Ericsson J. SREBP in signal transduction: cholesterol metabolism and beyond. Curr Opin Cell Biol. 2007; 19:215–222. [PubMed: 17303406]
39. Guo R, Wan CK, Carpenter JH, Mousallem T, Boustany RM, Kuan CT, et al. Synergistic control of T cell development and tumor suppression by diacylglycerol kinase alpha and zeta. Proc Natl Acad Sci U S A. 2008; 105:11909–11914. [PubMed: 18689679]
40. Kay MA, Glorioso JC, Naldini L. Viral vectors for gene therapy: the art of turning infectious agents into vehicles of therapeutics. Nat Med. 2001; 7:33–40. [PubMed: 11135613]

NIH-PA Author Manuscript

NIH-PA Author Manuscript

NIH-PA Author Manuscript

41. Roller DG, Axelrod M, Capaldo BJ, Jensen K, Mackey A, Weber MJ, et al. Synthetic lethal screening with small-molecule inhibitors provides a pathway to rational combination therapies for melanoma. Mol Cancer Ther. 2012; 11:2505–2515. [PubMed: 22962324]

42. Lee J, Kotliarova S, Kotliarov Y, Li AG, Su Q, Donin NM, et al. Tumor stem cells derived from glioblastomas cultured in bFGF and EGF more closely mirror the phenotype and genotype of primary tumors than do serum-cultured cell lines. Cancer Cell. 2006; 9:391–403. [PubMed: 16697959]

43. Folch J, Lees M, Sloane Stanley GH. A simple method for the isolation and purification of total lipides from animal tissues. J Biol Chem. 1957; 226:497–509. [PubMed: 13428781]

44. Neschen S, Morino K, Hammond LE, Zhang D, Liu ZX, Romanelli AJ, et al. Prevention of hepatic steatosis and hepatic insulin resistance in mitochondrial acyl-CoA:glycerol-sn-3-phosphate acyltransferase 1 knockout mice. Cell Metab. 2005; 2:55–65. [PubMed: 16054099]

45. Nagle CA, An J, Shiota M, Torres TP, Cline GW, Liu ZX, et al. Hepatic overexpression of glycerol-sn-3-phosphate acyltransferase 1 in rats causes insulin resistance. J Biol Chem. 2007; 282:14807–14815. [PubMed: 17389595]

46. Murphy RC, James PF, McAnoy AM, Krank J, Duchoslav E, Barkley RM. Detection of the abundance of diacylglycerol and triacylglycerol molecular species in cells using neutral loss mass spectrometry. Anal Biochem. 2007; 366:59–70. [PubMed: 17442253]

47. http://www.acdlabs.com/))

NIH-PA Author Manuscript

NIH-PA Author Manuscript

NIH-PA Author Manuscript

SIGNIFICANCE

Diacylglycerol kinase alpha (DGKα), which converts diacylglycerol to phosphatidic acid, regulates critical oncogenic pathways, notably HIF-1α and mTOR. DGKα knockdown and small-molecule inhibition are selectively toxic to human cancer cells but not normal human cells, and DGKα inhibition slows tumor growth, decreases angiogenesis, and increases mouse survival in xenograft models.

NIH-PA Author Manuscript
NIH-PA Author Manuscript
NIH-PA Author Manuscript

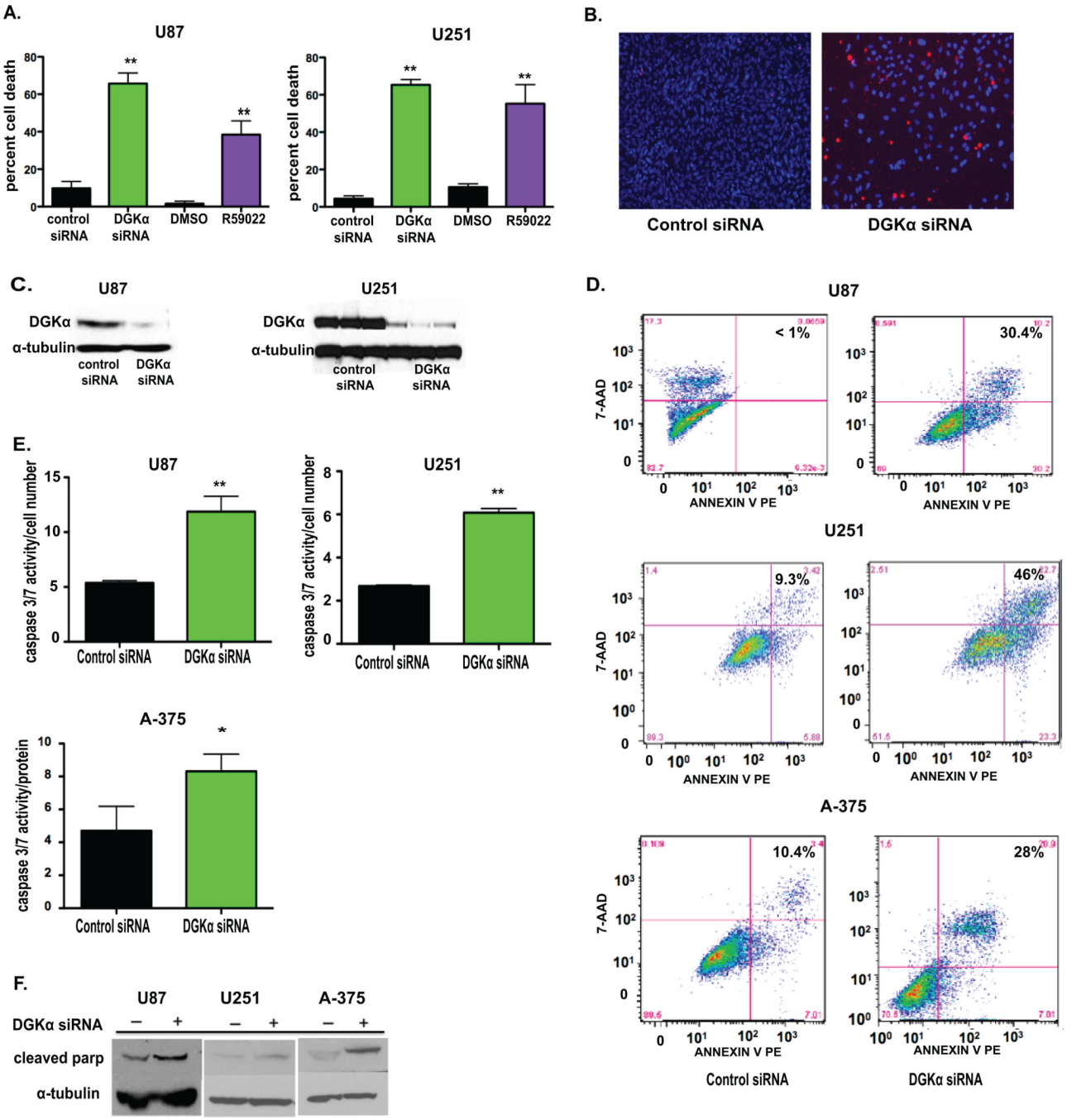

Figure 1. DGKα inhibition causes toxicity in glioblastoma and melanoma cells

A, DGKα knockdown was assessed in GBM cells U87 and U251 via transfection with either control or DGKα siRNA and inhibition via treatment with DMSO (v:v) or R59022 at 10 μM. Percent cell death was evaluated after 4 days. **B**, To visualize cell death changes after DGKα knockdown, U251 GBM cells were stained with Hoechst and propidium iodide. **C**, An immunoblot was used to verify transfection efficiency with siRNA in U87 and U251 cell lysates at 72 hours with α-tubulin as control. **D**, FACS analysis was performed on both U87, U251, and A-375 cell lines showing an increase in Annexin V-stained cells after DGKα knockdown. E, Caspase 3/7 activity was measured 36–72 hours after DGKα knockdown in

U87, U251, and A-375 melanoma cells. **F**, Protein levels of cleaved PARP were also increased in U251, A-375, and U87 cells after DGKα silencing. (*, P<0.05 and **, P<0.01, Student t test)

NIH-PA Author Manuscript
NIH-PA Author Manuscript
NIH-PA Author Manuscript

NIH-PA Author Manuscript
NIH-PA Author Manuscript
NIH-PA Author Manuscript

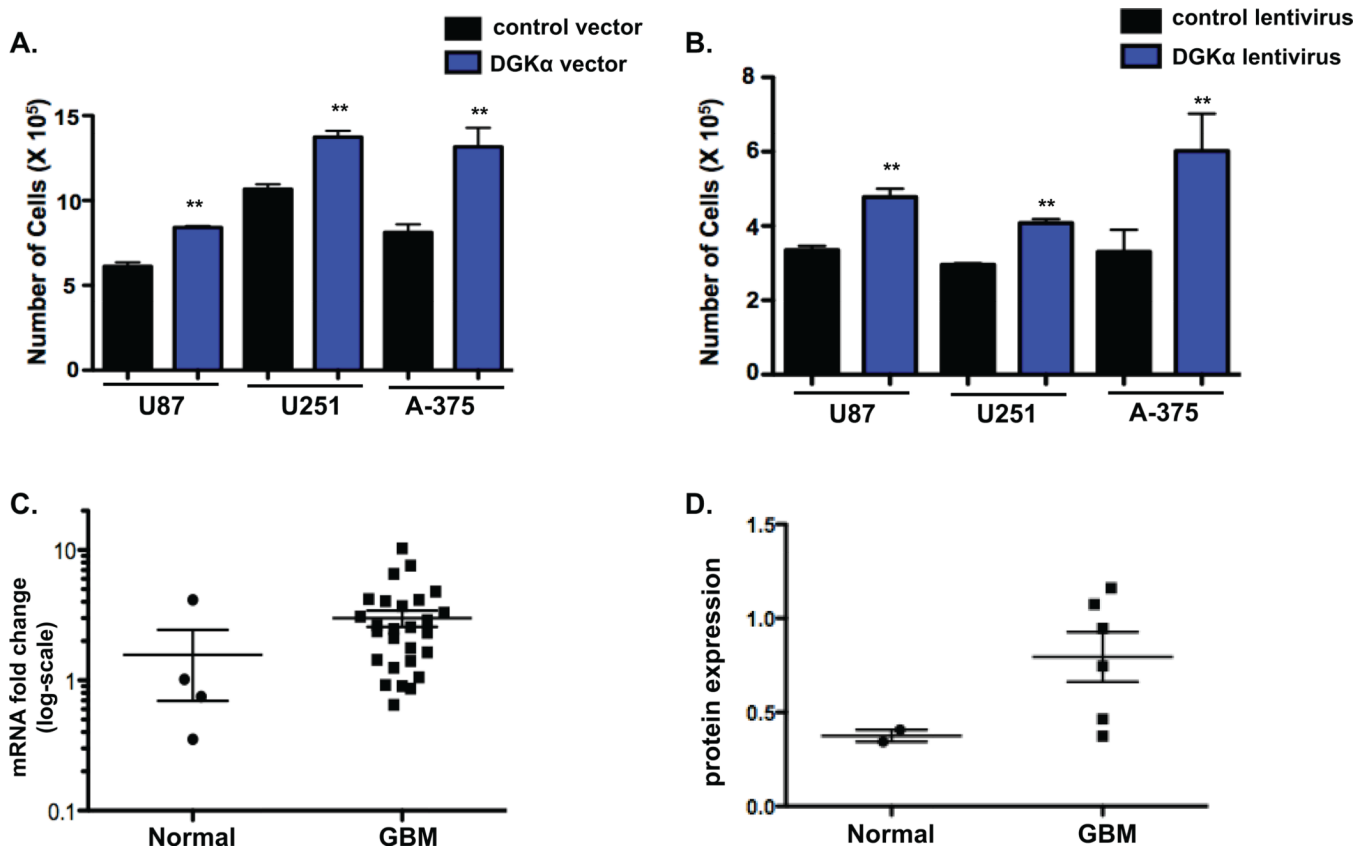

Figure 2. DGKα is up-regulated in GBM and increases cell numbers

A, Cell numbers for U87 and U251 glioblastoma and A-375 melanoma cells were assessed 72 hours after over-expression of DGKα by plasmid transfection versus control plasmid (TOPO-TA plasmid, Invitrogen). **B**, DGKα was over-expressed via lentiviral infection in U87, U251 and A-375 cells to assess the effect on cell proliferation when compared to control cells. **C**, DGKα levels in human tissue samples were evaluated by measured intensity of immunoblot in GBM samples and compared to normal brain after normalizing by the ratio of DGKα intensity to α-tubulin intensity. **D**, DGKα mRNA levels were quantified by qRT-PCR and normalized by 18S RNA in normal versus GBM human tissue samples. The scatterplot exhibits the trend toward increased mRNA fold expression in GBM samples. (*, $P<0.05$ and **, $P<0.01$ Student t test)

NIH-PA Author Manuscript
NIH-PA Author Manuscript
NIH-PA Author Manuscript

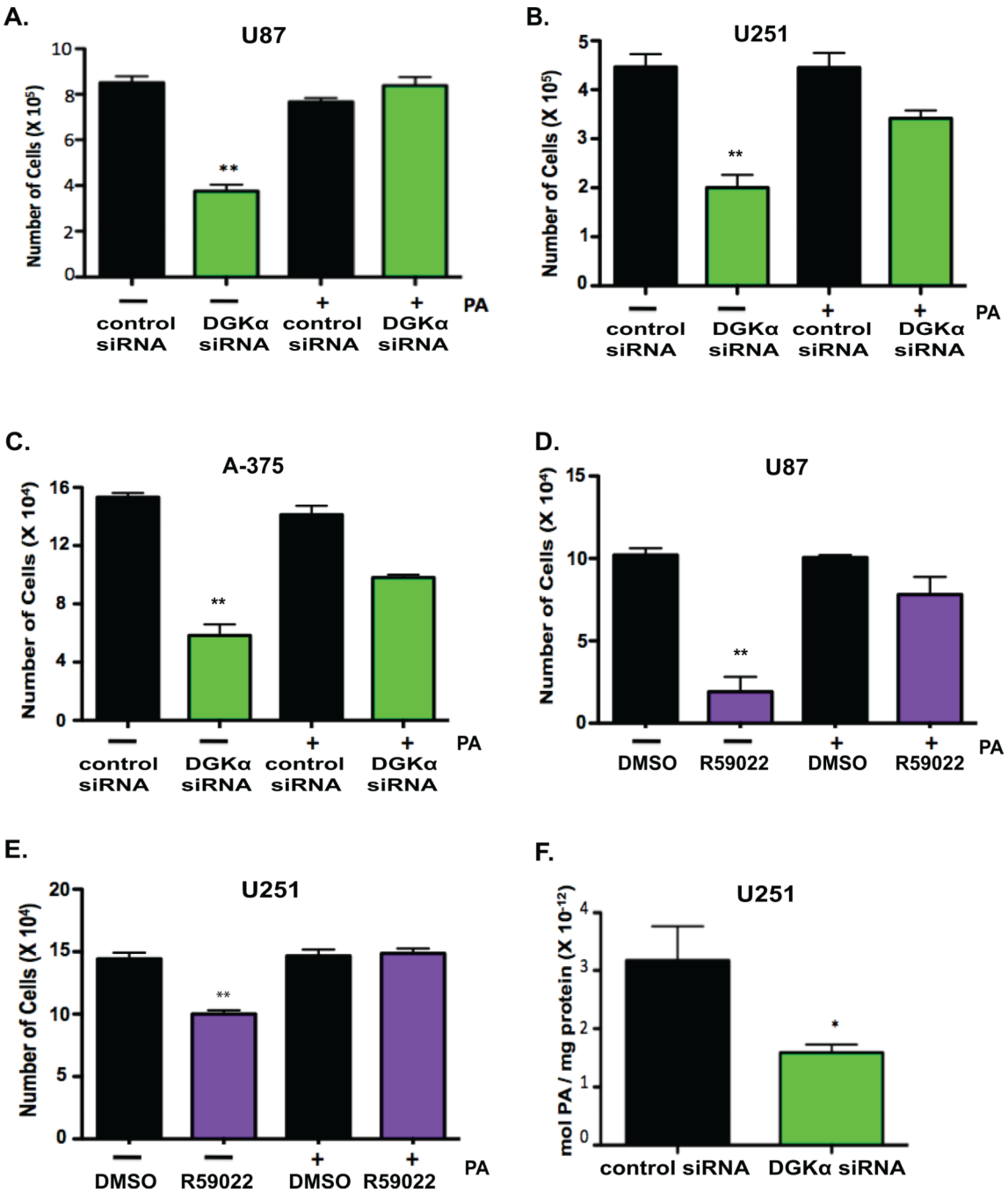

Figure 3. DGKα inhibition and phosphatidic acid synthesis

A, U87 and **B**, U251 GBM cells, and **C**, A-375 melanoma cells were transfected with control or DGKα siRNA with simultaneous administration of exogenous PA at 33 μM or vehicle (1 MeOH : 2 Chloroform, v:v). Full phenotypic rescue of decreased cell viability was observed upon delivery of PA to DGKα siRNA transfected cells. Phenotypic rescue was achieved in **D**, U87 and **E**, U251 GBM cells treated with R59022 at 5 μM. **F**, After transfection with siRNA, mass spectrometry was utilized to show a decrease in total PA levels in lipid lysates from U251 cells. (*, $P<0.05$ and **, $P<0.01$ Student t test)

NIH-PA Author Manuscript
NIH-PA Author Manuscript
NIH-PA Author Manuscript

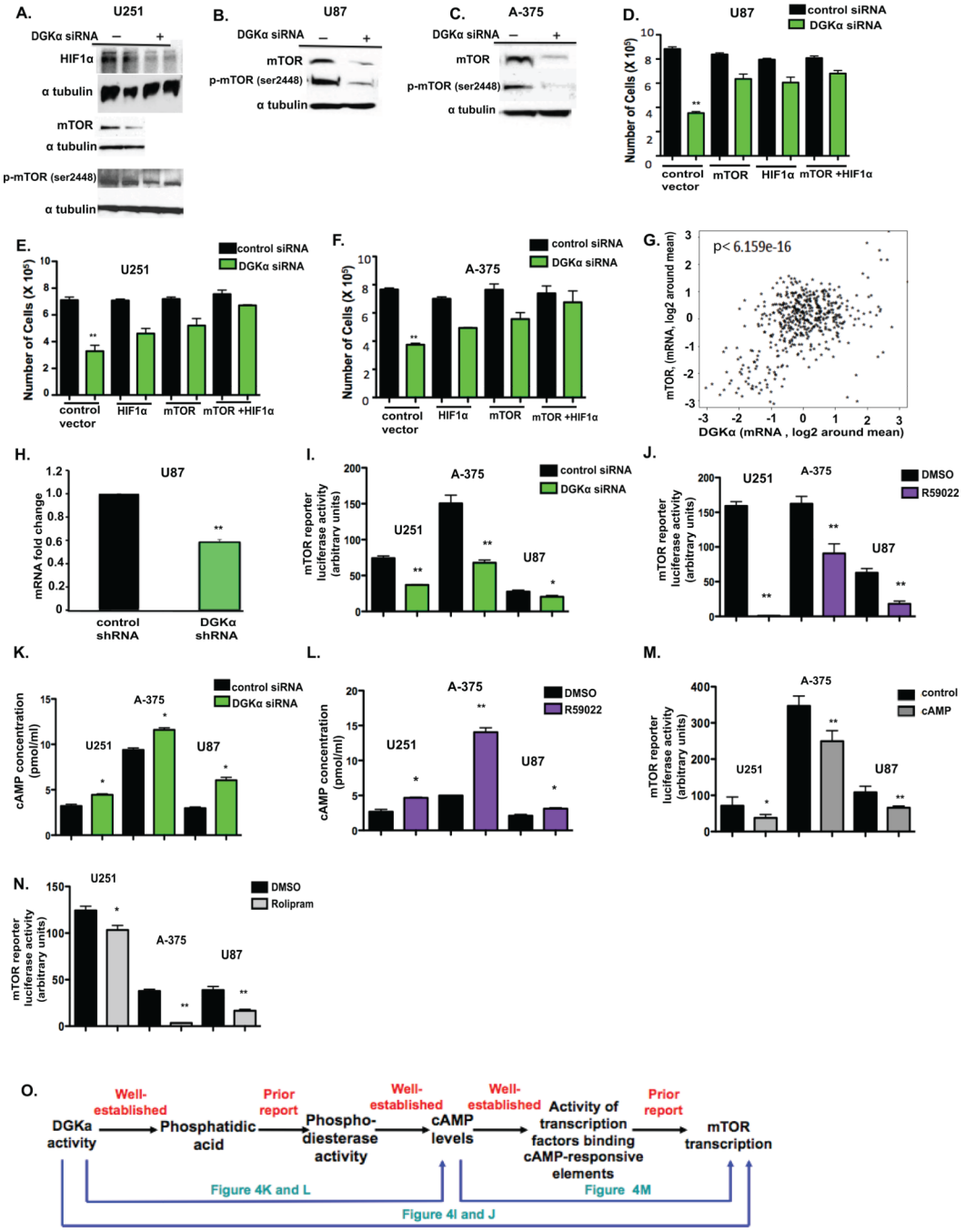

Figure 4. DGKα induces glioblastoma cell death through regulating oncogenic pathways

A, Immunoblot analysis of HIF-1α, total mTOR, and phos-mTOR$_{ser2448}$ in U251 cells transfected with DGKα or control siRNA. **B**, Total mTOR and phos-mTOR$_{ser2448}$ were decreased in U87 cell lysates, as well as in **C**, A-375 cell lysates. To verify the role HIF-1α and mTOR play in the observed cell toxicity, each was over-expressed through plasmid transfection and cell proliferation was assayed in **D**, U87 cells, **E**, U251 cells, and **F**, A-375 cells transfected with siRNA. **G**, Plot of *DGKA* versus *mTOR* mRNA expression levels in 576 human GBM samples (15). Spearman's correlation test performed with a p-value of $6.159e^{-16}$ and a Pearson's correlation test p-value of $< 2.2e^{-16}$. **H**, In U87, mRNA levels of

NIH-PA Author Manuscript

NIH-PA Author Manuscript

NIH-PA Author Manuscript

mTOR were quantified by qRT-PCR in response to DGKα knockdown via shRNA and fold expression changes in comparison to control shRNA are shown. In U251, U87, and A-375 cells the effects of **I**, DGKα knockdown via siRNA and **J**, inhibition via small-molecule inhibitor on mTOR transcription were evaluated through mTOR promoter luciferase activity assay. **K and L**, levels of predicted mediator cAMP were measured by ELISA after attenuation of DGKα by siRNA (**K**) or inhibitor (**L**) in U251, U87 and A-375 cells. **M**, the addition of exogenous cAMP at 20 and 80 pmol, and **N**, PDE4 inhibitor rolipram at 40 μM were observed to affect mTOR transcription by reporter assay. **O**, A schematic of the proposed pathway of DGKα regulation of mTOR transcription. (*, $P<0.05$ and **, $P<0.01$ Student t test)

NIH-PA Author Manuscript
NIH-PA Author Manuscript
NIH-PA Author Manuscript

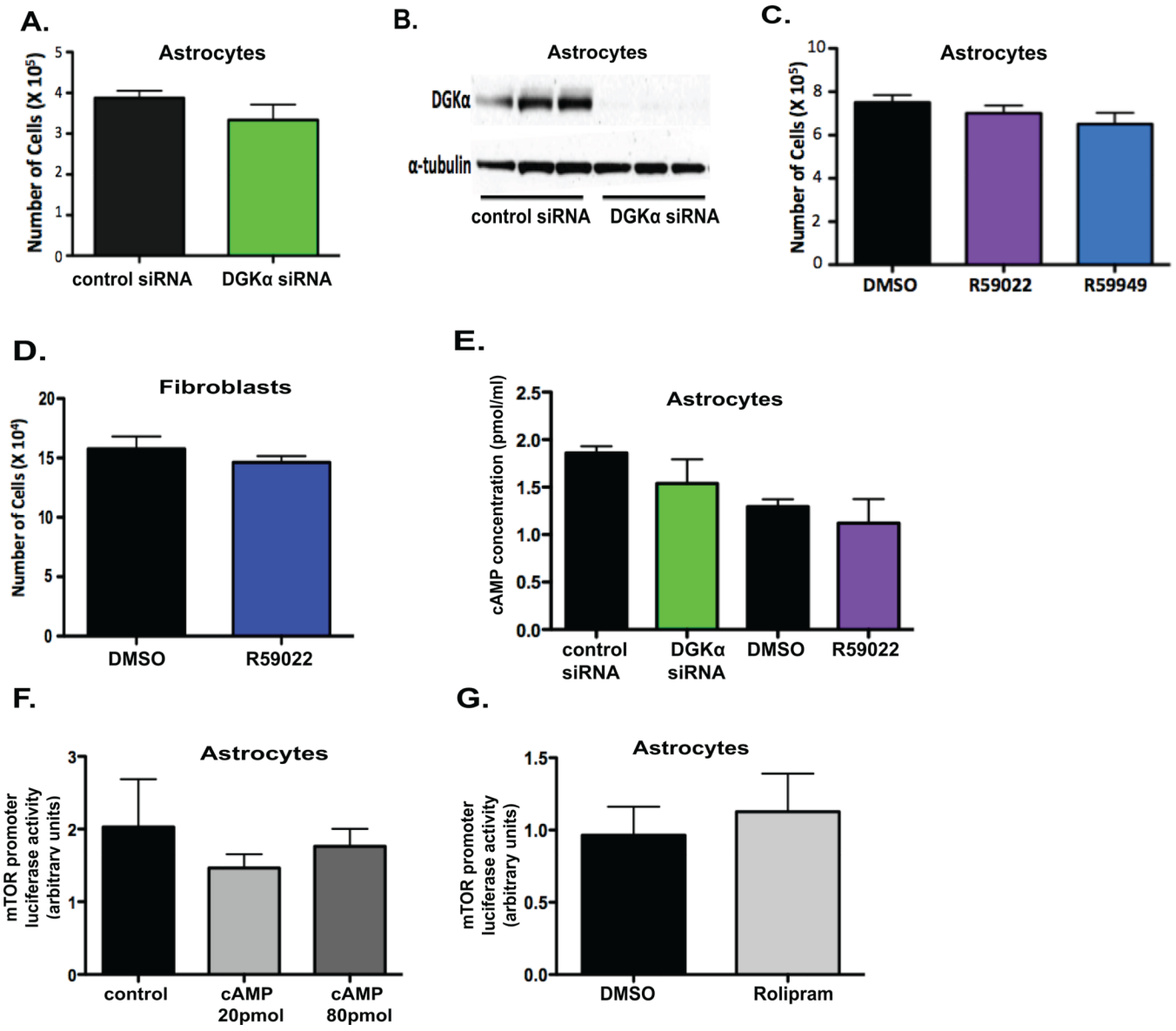

Figure 5. DGKα attenuation is safe in normal cells

A, Normal human astrocytes were transfected with either control or DGKα siRNA, and cell number was assessed at 3 days post transfection. **B**, An immunoblot was done on cell lysates post-transfection to check for transfection efficiency. **C and D**, Normal human astrocytes and fibroblasts were treated with 10 μM R59022, R59949, or DMSO (v:v) control and cell proliferation was assessed at 3 days post treatment, with no significant decrease observed in cell number. **E**, Levels of cAMP were also evaluated via ELISA 5 days after knockdown and inhibition of DGKα in astrocytes. **F**, Effects of exogenous cAMP on mTOR transcription in astrocytes were assessed through mTOR promoter luciferase assay 5 days after treatment. **G**, Rolipram was administered at 40 μM to further test the effect of phosphodiesterase inhibition/cAMP levels on mTOR transcription in astrocytes, with promoter activity assayed at 6 days post treatment. (*, P<0.05 and **, P<0.01 Student t test)

NIH-PA Author Manuscript

NIH-PA Author Manuscript

NIH-PA Author Manuscript

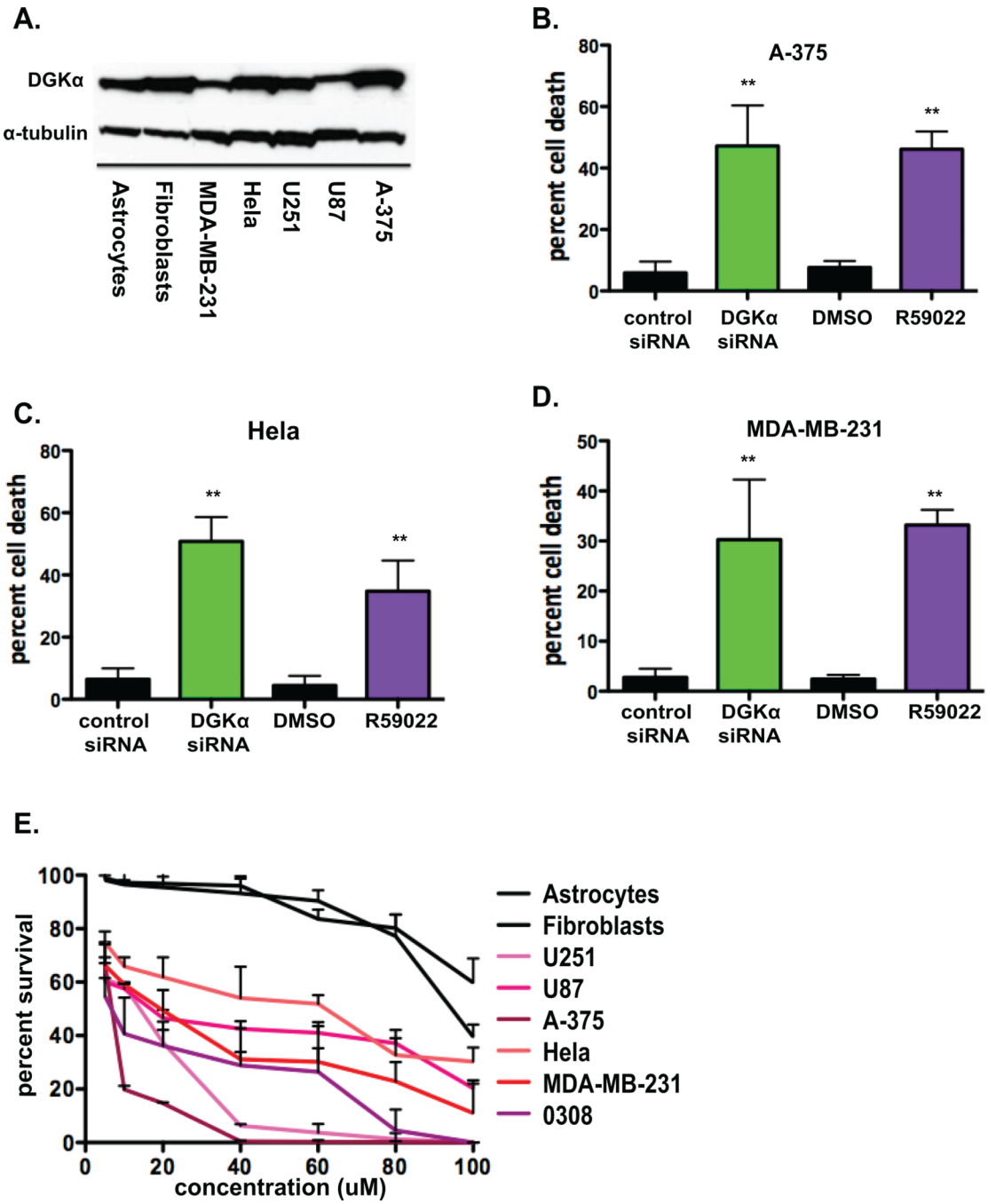

Figure 6. Attenuation of DGKα activity has preferential toxicity for cancer cell line

A, Basal DGKα levels were evaluated by immunoblot in normal human cell lines and various cancer cell lines, with α-tubulin shown as loading control. Cell toxicity was assessed by cell counts/trypan blue in **B**, A-375 (melanoma), **C**, HeLa (cervical cancer), and **D**, MDA-MB-231 (breast cancer) lines 4 days after DGKα knockdown or treatment with R59022 at 10 μM or DMSO vehicle. **E**, Dose response curves were generated for astrocytes, fibroblasts, U251, U87, A-375, HeLa, MDA-MB-231, and 0308 (GBM stem cell) cells by cell counts and normalized for DMSO (v:v) at 5, 10, 20, 40, 60, 80, and 100 μM R59022 after 4 days of treatment. (*, P<0.05 and **, P<0.01 Student t test)

NIH-PA Author Manuscript
NIH-PA Author Manuscript
NIH-PA Author Manuscript

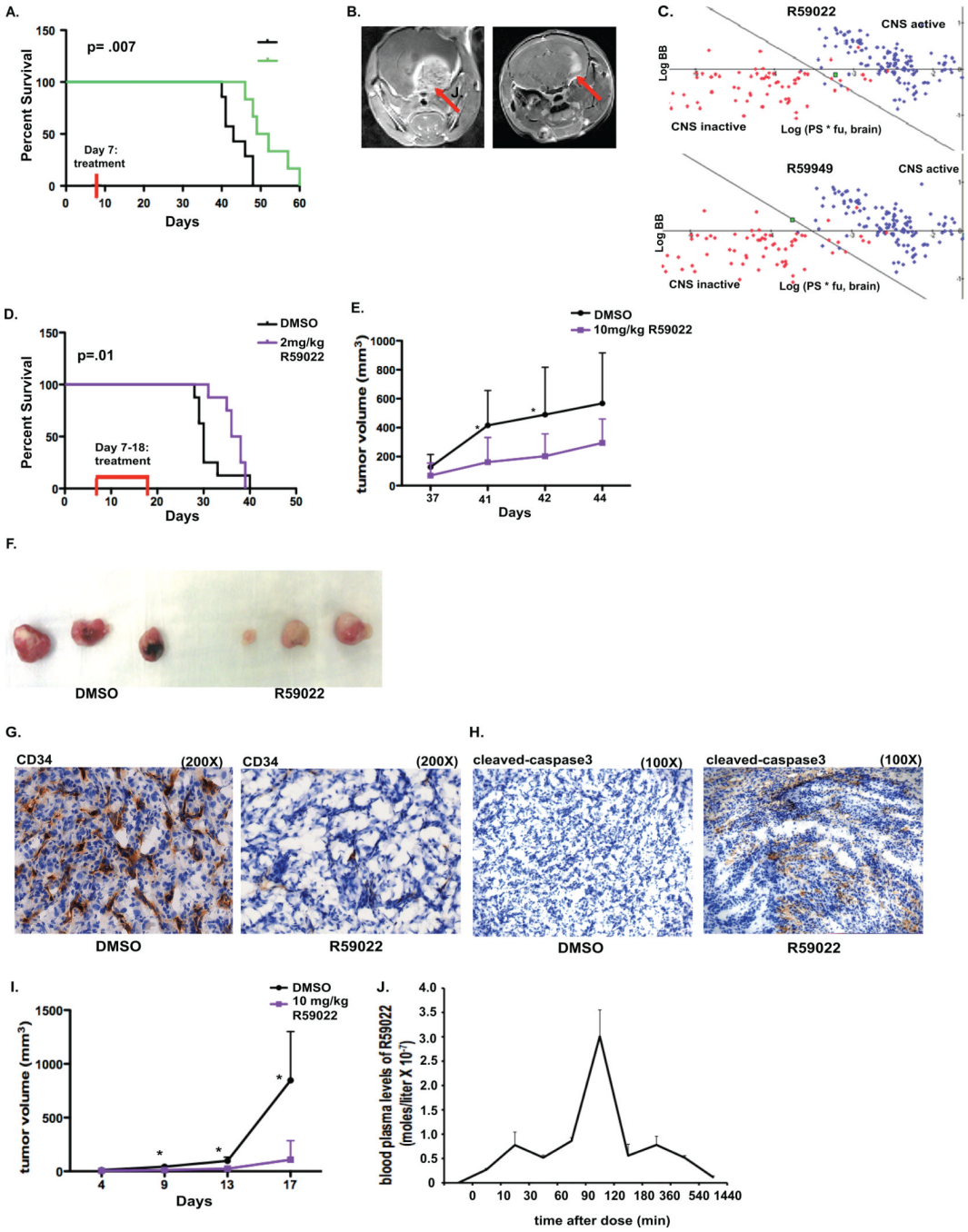

Figure 7. DGKα knockdown and inhibition affect *in vivo* tumor growth, angiogenesis, and mouse survival

A, After *in vivo* implantation of 0308 GBM stem cells and CED infusion of lentiviral particles with control or DGKα shRNA one week later, mouse survival was followed. A Kaplan-Meier curve and log-rank analysis exhibits a significant increase in survival of mice in the treatment group when compared to control mice (p=.007). **B**, MRIs were conducted at 40 days post tumor implantation and show characteristically smaller tumors in mice in the treatment group. **C**, Plot of CNS activity presents several known CNS-penetrating (blue points) and peripherally acting (red points) drugs, with the green points denoting either DGKα inhibitor R59022 or R59949. **D**, Mice were injected with U87 intracranially and then

NIH-PA Author Manuscript

NIH-PA Author Manuscript

NIH-PA Author Manuscript

treated with daily IP injections of R59022 or vehicle on days 8 through 19. IP injections of R59022 at 2 mg/kg significantly increased median survival (p=.01) compared to DMSO (v:v) controls. (* p<0.01 log-rank analysis). **E**, Tumor volume of subcutaneous U87 tumors *in vivo* was assessed after daily treatment with either R59022 10 mg/kg or vehicle, with treatment beginning 37 days after tumor implantation. **F**, Subcutaneous U87 tumors were resected and exhibited a visible difference in vascularity after treatment with R59022 versus vehicle and **G**, frozen sections were stained for CD34 to assess for blood vessels after treatment (magnification of 200X). **H**, Immunohistochemistry was done for cleaved caspase-3 to assess apoptosis in the resected tumors above (magnification of 100X). **I**, Tumor volume of subcutaneous A-375 tumors *in vivo* was evaluated after daily treatment with DMSO or R59022 at 10 mg/kg starting 4 days after tumor implantation. **J**, To evaluate the pharmacokinetics of R59022 *in vivo*, after a single IP dose of R59022 blood was collected at various time points via cardiac puncture, with the samples used for mass spectrometry for blood plasma levels of R59022. (*, P<0.05 and **, P<0.01 Student t test)